Positioning of Salt Gradients in Ion-Exchange SMB

Joukje Houwing, Thomas B. Jensen, Stef H. van Hateren, Hugo A. H. Billiet, and Luuk A. M. van der Wielen
Kluyver Laboratory for Biotechnology, Delft University of Technology, 2628 BC Delft, The Netherlands

Salt gradients can be used to improve the efficiency of ion-exchange separations in simulated moving-bed systems. The gradient, formed by the use of feed and desorbent solutions of different salt concentrations, introduces regions of increased and decreased affinity of, for example, proteins for the matrix. Several gradient shapes can be formed, depending on the flow-rate ratios and salt concentrations used. Only some of these effectively increase throughput or decrease desorbent consumption. Correct gradient positioning is essential, but not trivial, because salt is adsorbed in the resin. A procedure developed selects the flow-rate ratios that allow correct positioning of gradients based on wave theory and incorporates the nonlinear Donnan isotherm of salt on ion-exchange resins. Predictions are verified by experiments combined with a mathematical equilibrium stage (true moving-bed) model. Upward and downward gradients are compared with respect to the use of desorbent and salt.

Introduction

More and more, simulated moving-bed (SMB) systems are used for the separation of fine chemicals and pharmaceuticals. The countercurrent chromatographic process has been successfully applied for a more efficient separation of similar molecules, reduction of resin inventory, and a reduction of solvent consumption relative to conventional chromatographic processes (Juza et al., 2000; Van Walsem and Thomson, 1997; Ballanec and Hotier, 1993).

In earlier work, we have introduced the salt-gradient SMB. The gradient, a situation of high affinity above the feed and a low affinity below the feed, improves the separation of diluted protein mixtures by ion-exchange chromatography (Houwing et al., 1997, 1999). In protein separations, salt is often used to manipulate the affinity of proteins for the ion-exchange resin (Kopaciewitz et al., 1989). The affinity is reduced at increased salt concentration. Thus, different salt concentrations in the feed and desorbent of an SMB can introduce regions of high and low affinity (Figure 1). The high-affinity situation above the point of feed introduction enables the loading of a large volume of feed. The low affinity below the feed point facilitates elution of the protein. Thus, compared to the isocratic situation, throughput is increased, whereas solvent consumption is decreased. Only few references on gradients in SMB systems have been found in the literature. These include the use of temperature gradients for the separation of amino acids (Ruthven and Ching, 1989) and

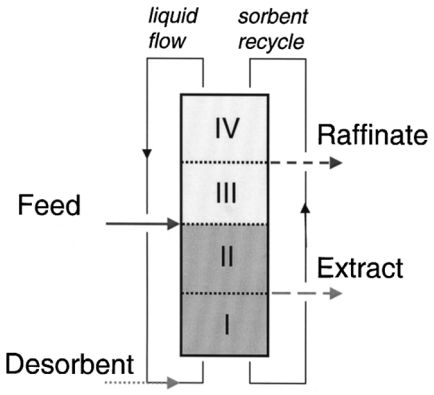

Figure 1. Gradient in an SMB system.
The darker gray indicates an increased salt concentration, that is, a decreased affinity.

Correspondence concerning this article should be addressed to L. A. M. van der Wielen.

enantiomeric amino-acid derivatives (Migliorini et al., 2001), pressure gradients in supercritical fluid SMB (Mazzotti et al., 1997), and gradients in solvent strength in reversed-phase chromatography (Jensen et al., 2000).

In previous work (Houwing et al., 1997, 1999), we have assumed that the sorbent is saturated with salt, independent of the location in the SMB. However, salt may adsorb unto the resin in a concentration dependent manner (Jansen et al., 1996). Then the positioning of the gradient is no longer straightforward. The distribution of salt over the two phases, which depends on the location in the system, needs to be computed similarly to that of any adsorbing component. The movement of salt should thus be considered for a correct flow-rate selection. Several procedures have been described for the selection of the relative liquid to sorbent flow rates in SMB systems. These rely on the true moving-bed (TMB) comparison with the simulated moving bed, that is, where both sorbent and solvent move. The most important procedures are based on the wave theory. "Triangle theory" is based on the net flow of components and uses a mathematical transformation (omega transform) (Storti et al., 1993). A similar approach, without transformation, is suggested by Ma and Wang (1997). Also, McCabe Thiele analysis is used for flow selection (Ruthven and Ching, 1989).

This article starts with a description of a typical isotherm of salt on an ion-exchange resin. This isotherm is used in the procedure for positioning of the salt gradient in the SMB, based on the wave theory. Experimental results that confirm the theory are shown. The article concludes with a comparison of upward and downward gradients with respect to solvent and salt use.

Theory

Salt isotherm

For the description of the behavior of salt solutions on ion-exchange resins, we draw a parallel to membrane science. In nanofiltration, a charged membrane is used to separate charged ionic species. At low salt concentrations, the coions, that is, ions of like charge as the membrane, do not enter the membrane, due to ionic repulsion. This is also known as "Donnan exclusion." At increased salt concentrations, the coion also passes the membrane, as the electrical shielding extends over a shorter range at increased ionic strength (Mulder, 1991).

A similar phenomenon has been observed in ion-exchange chromatography (Jansen et al., 1996). At low salt concentration, only the counterions enter the resin and are exchanged, whereas the coions are excluded. However, at increased concentration, the integral salt molecule is taken up as a result of the reduced charge effects.

Consider an ion-exchange resin of capacity Q that is contacted with a solution of sodium chloride at molarity c. The concentration of ions in the sorbent and liquid at equilibrium can be calculated by equating the chemical potentials of ion, i, in the two phases

$$\Delta\mu_i^0 + RT\ln\frac{x_i}{y_i} + z_i F\Delta\Psi = 0 \qquad (1)$$

where $x_i = c_i/Q$, $y_i = q_i/Q$, z_i is the charge of ion i, $\Delta\mu^0$ denotes the difference in the standard chemical potential of the liquid to the sorbent phase, and $\Delta\Psi$ is the electrical potential difference of liquid to the sorbent phase. In the derivation, it has been assumed that the solutions behave ideally thermodynamically and that swelling effects can be neglected. Since both sodium and chloride experience the same potential difference, $\Delta\Psi$ is eliminated by the addition of the two-component balances. The result is

$$\frac{y_{\mathrm{Cl}}}{x_{\mathrm{Cl}}} = S\frac{x_{\mathrm{Na}}}{y_{\mathrm{Na}}} \qquad (2)$$

where

$$S = \exp\left(\frac{\Delta\mu^0_{\mathrm{Na}} + \Delta\mu^0_{\mathrm{Cl}}}{RT}\right)$$

The quantity S is a selectivity coefficient, which is similar to the selectivity coefficient during the uptake of two counterionic species.

The concentrations of sodium and chloride are related by the electroneutrality equations for liquid and sorbent phase

$$\begin{aligned} &\text{liquid:} && x_{\mathrm{Na}} = x_{\mathrm{Cl}} \\ &\text{sorbent:} && 1 + y_{\mathrm{Na}} = y_{\mathrm{Cl}} \end{aligned} \qquad (3)$$

Substitution of Eq. 3 in Eq. 2 leads to

$$y_{\mathrm{Na}} = -\frac{1}{2} + \frac{1}{2}\sqrt{1 + 4Sx^2_{\mathrm{Na}}} \qquad (4)$$

At low concentrations, salt is predicted to be excluded from the resin, whereas at high concentrations, it is taken up proportionally to the salt concentration, with a proportionality constant that equals the square root of the selectivity (Figure 2). This isotherm shape results in diffuse breakthrough fronts

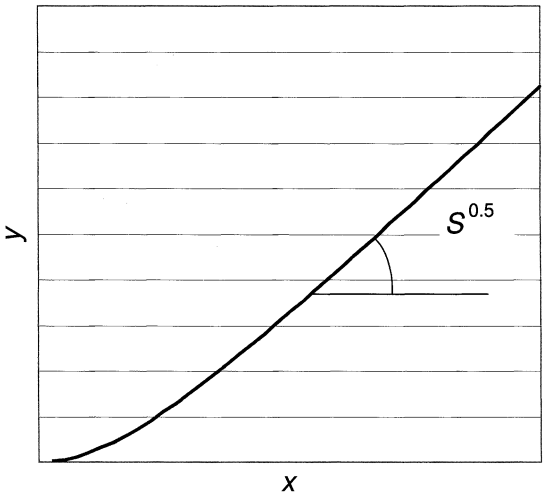

Figure 2. Donnan-based isotherm of salt on an ion-exchange resin.

during the loading of a column with increasing concentrations as well as sharpening breakthrough fronts during elution with decreasing concentrations (Helfferich and Klein, 1970).

Upward and downward movement

Any component present in the SMB is moved in a certain direction relative to the fixed inlets and outlets. In fact, it is not the component that is moved, but the fronts between the loaded and unloaded portions of the column. The direction and rate of movement can be determined from wave theory; the front velocity (w) in the countercurrent separation system is calculated from (Rhee et al., 1971)

$$w = \frac{v_s \beta \left(m - \dfrac{\partial q}{\partial c} \right)}{\left(1 - \beta \dfrac{\partial q}{\partial c} \right)} \tag{5}$$

where v_s is the interstitial solids velocity; β is the column phase ratio ($=(1-\epsilon)/\epsilon$), where ϵ is the column porosity; $m = \Phi_L/\Phi_S$ indicates the flow-rate ratio of liquid to resin phase; and $\partial q/\partial c$ is the slope of the isotherm. In the case of shock waves, all $\partial q/\partial c$ are replaced by $\Delta q/\Delta c$, the chord of the isotherm.

A positive wave velocity indicates upward movement (cf. Figure 1). Hence, upward movement will only occur when the numerator is of a positive sign, that is, when the value of m exceeds the local slope $\partial q/\partial c$ (in the case of a diffuse wave) or chord $\Delta q/\Delta c$ (in the case of a sharpening wave) of the isotherm.

Gradient shapes

Salt is an adsorbing component. Hence, the fronts that determine the gradient can move both upward and downward. Thus, gradients can occur in different shapes and can be formed from different starting conditions. For reasons of clarity, let us define the gradient shapes:

- A "top gradient" is the situation of high affinity above the feed and low affinity below the feed.
- A "bottom gradient" is the situation of low affinity above the feed and high affinity below the feed.
- An "upward gradient" is the situation where the salt is transported predominantly by the liquid phase.
- A "downward gradient" is the situation where the salt is transported predominantly by the sorbent phase.

In the previous work (Houwing, 1997, 1999), we have discussed the most obvious form of the gradient, the "upward top" gradient (Figure 3). A desorbent of high salt concentration and a feed solution of lower salt concentration are used. This situation is only possible at low affinity of the salt or at high flow-rate ratios, that is, where salt is transported predominantly by the liquid.

A less obvious form of the gradient, the "downward top" gradient occurs when there is a strong interaction between salt and the ion-exchange resin and flow-rate ratios are relatively low. Salt is then predominantly transported by the sorbent. The top gradient is formed by the use of a low salt concentration in the desorbent and a high salt concentration in the feed.

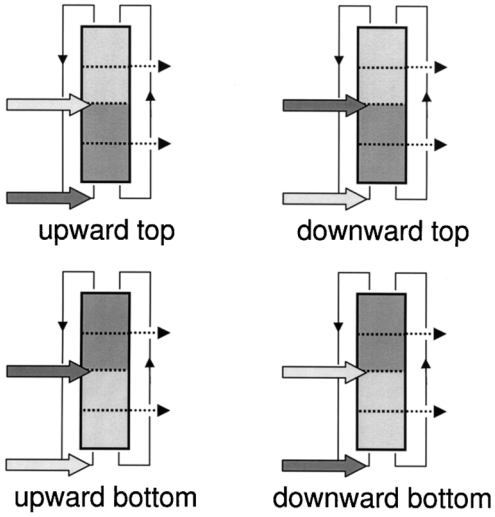

Figure 3. Gradient shapes.

The darker gray indicates a high concentration of salt, that is, a low affinity of proteins for the matrix.

"Bottom" gradients can be formed similarly. An "upward bottom" gradient is formed using concentrated feed and less concentrated desorbent at flow-rate ratios that allow upward motion. The "downward bottom" gradient is formed using concentrated desorbent and less concentrated feed at flow-rate ratios that allow downward transport. However, only the "top" gradients have the desired effect of improving the loading capacity and reducing solvent consumption. The bottom gradient is very unfavorable, since the low affinity in the top sections reduces the loading capacity of the adsorbent and the high affinity in the bottom sections increases solvent consumption. In the following, we will consider only the top gradients.

Positioning of gradient

In order to correctly position the gradient, the relative liquid-to-sorbent flow-rate ratios need to be chosen carefully. The procedure to estimate these flow ratios is based on wave theory (Helfferich and Klein, 1970; Rhee et al., 1971) and is similar to the procedures suggested by Storti et al. (1993) and Ma and Wang (1997). The basis is the wave-velocity equation (Eq. 5), where the flow-rate ratios are adjusted to assure upward or downward movement.

The procedure can be summarized as follows:

(1) Define the concentrations at the lower (L) and upper (U) side of the fronts. The lower side of the front is the side nearest to the lower section number (cf. Figure 1).

(2) Realize the shape of the front: shock fronts or spreading fronts may occur as a result of the nonlinear isotherm.

(3) Calculate the front velocity from wave theory and adjust the flow-rate ratios such that upward or downward movement is assured.

Step 1: Defining Concentrations. The concentrations occurring in the SMB are governed by the flow rates used. The profiles in the SMB can be drawn qualitatively beforehand. In the following, we will only consider an "open-loop system," where the liquid leaving section IV is not recycled to section I.

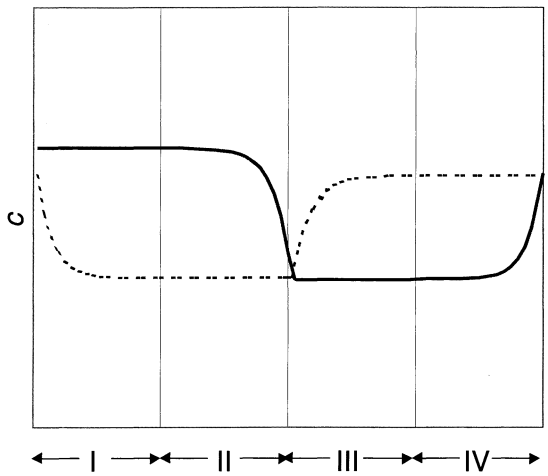

Figure 4. Profile in an equivalent TMB at an upward (drawn line) and downward (dashed line) gradient.

Roman numerals indicate section numbers.

In the case of an upward gradient, the lower sections (I and II) of the SMB are saturated with the desorbent. At the point of feed introduction, the feed solution and the stream leaving section II are mixed, leading to a lower concentration, which will extend throughout sections III and IV.

The change in concentration at the feed point cannot be abrupt, as a result of dispersion as well as of local nonequilibrium at the feed position. Thus, there is a gradual decrease in concentration just below the feed inlet. The gradual decrease cannot occur above the feed, because it would then immediately be transported through the column, just like any front. A similar situation occurs at the desorbent inlet. An indicative drawing is shown in Figure 4.

In the case of a downward gradient, sections III and IV are at a higher concentration. The gradual transitions in concentrations are located just above the feed and desorbent point, as indicated in Figure 4. No change in concentration is seen just below these points, since any change in concentration is immediately transported downward as a new front.

For a quantitative description of the concentrations, mass balances need to be solved. In the case of the upward gradient, there is one unknown concentration, namely, the concentration in sections III and IV. It can be calculated as a function of m_3 from a mass balance over the feed position

$$m_2 c_D + (m_3 - m_2) c_F - m_3 c_{\mathrm{III}} + q_{\mathrm{III}} - q_D = 0 \qquad (6)$$

where c_F and c_D are the feed and desorbent concentrations, respectively, and q_D is the resin phase concentration in equilibrium with the desorbent. Equilibrium is assumed to be reached in all sections (cf. Storti et al., 1993); hence, the solid-phase concentration in section j can be calculated from the corresponding liquid-phase concentration from the isotherm. This equation differs from the one used in previous work (Houwing et al., 1999), where the terms q_{III} and q_D cancel because of the assumed constant saturation of the resin.

In the case of a downward gradient, there are two unknown concentrations, namely, the concentrations at saturation in the major part of section I and section II (c_{II}) and the major part of section III and section IV (c_{IV}). They can be obtained from the mass balance over the feed point, combined to the mass balance over the desorbent point.

The mass balance over the feed point reads

$$m_2 c_{\mathrm{II}} + (m_3 - m_2) c_F - m_3 c_{\mathrm{IV}} + q_{\mathrm{IV}} - q_{\mathrm{II}} = 0 \qquad (7)$$

where q_{II} and q_{IV} are the sorbent concentrations in equilibrium with c_{II} and c_{IV}, respectively.

The mass balance over the desorbent point reads:

$$m_3 c_{\mathrm{IV}} - (m_4 - m_3) c_R - m_4 c_W + m_1 c_D - m_2 c_{\mathrm{II}} - (m_1 - m_2) c_E + q_{\mathrm{II}} - q_{\mathrm{IV}} = 0 \qquad (8)$$

The quantities c_E, c_R, and c_W are the concentrations at the extract, raffinate and waste stream, respectively. No front exists between section II and the extract outlet. Nor does a front exist between section IV and the waste outlet, or between section IV and the raffinate outlet (cf. Figure 4), so

$$c_E = c_{\mathrm{II}}$$
$$c_R = c_W = c_{\mathrm{IV}} \qquad (9)$$

Then, the mass balance over the desorbent point can be rewritten as

$$m_1 (c_D - c_{\mathrm{II}}) + q_{\mathrm{II}} - q_{\mathrm{IV}} = 0 \qquad (10)$$

By this procedure, all important concentrations are defined as a function of m.

Step 2: Identification of Waves. The wave velocity, Eq. 5, depends on the shape of the wave. In the case of the Donnan isotherm, the loading of a fixed-bed column with increasing salt concentrations results in diffuse waves, whereas the elution of a column with decreasing concentration results in shock waves (Helfferich and Klein, 1970), as has already been indicated. This also occurs in the case of SMB systems (Rhee et al., 1971; Storti et al., 1989). A wave is a shock wave when a lower concentration displaces a higher concentration relative to the direction of liquid flow, whereas a diffuse wave will occur in the reverse situation.

Step 3: Calculation of Front Velocity and Determination of Flow-Rate Ratio. Once the concentrations and shapes of the fronts are identified, the flow-rate ratios required for upward or downward movement can easily be calculated using Eq. 5.

The results of steps 1 through 3 are given in Table 1. In the case of the upward gradient, both fronts are bound by c_D and c_{III}. The entire spreading wave must have a positive velocity in sections I and II. Hence, the flow-rate ratios m_1 and m_2 have to exceed the maximal slope of the isotherm in the concentration interval, that is, at concentration, c_D. The shock

Table 1. Constraints on Flow-Rate Ratios for the Desired Gradients

	Front	c_L	c_U	Front shape	m
Upward	I	c_D	c_{III}	Spreading	$m_1,m_2 > (\partial q/\partial c)_{c_D}$
gradient	II	c_{III}	c_D	Shock	$m_3,m_4 > (\Delta q/\Delta c)_{c_D - c_{III}}$
Downward	I	c_D	c_{II}	Shock	$m_1,m_2 < (\Delta q/\Delta c)_{c_{II} - c_D}$
gradient	II	c_{II}	c_{IV}	Spreading	$m_3,m_4 < (\partial q/\partial c)_{c_{IV}}$

Source: After Storti et al., 1993.

wave in sections III and IV must also have a positive velocity, so the flow-rate ratios m_3 and m_4 need to exceed the chord of the isotherm. Similarly, in the case of the downward gradient, the shock wave bound by c_{II} and c_D in sections I and II must move downward, so m_1 and m_2 need to be smaller than the chord of the isotherm. The maximum, m, in sections III and IV is determined by the minimal slope in the concentration interval c_{II} to c_{IV}, that is, the slope at the maximum concentration, c_{IV}.

So far, the maximum or minimum flow-rate ratios are obtained as a function of the concentrations in the system, as summarized in the far right column of Table 1. The boundaries of an "operating region" (Storti et al., 1993) can be calculated by equating m to the limiting value and simultaneously solving this equation and the mass-balance equations over the feed and desorbent position (Eqs. 6, 7, and 10). The result is a restricted area, which defines the flow rates that can be used for correct positioning of the gradient.

Experimental

Materials

All salts were of analytical grade and were obtained from Merck. The sorbent, Q-Sepharose FF, was obtained from Amersham Pharmacia Biotech. This strong anion exchanger, based on highly cross-linked agarose has an average particle size of 90 μm and has a capacity for small ions of a 0.2-mol/L packed bed (Pharmacia Biotech, 1996). All solutions used were based on a 0.01-M tris buffer, pH 8.0.

Columns

Columns were prepared by packing the sorbent in empty columns according to the procedure described by the sorbent manufacturer. The sorbent was packed in 0.01-m-diameter Omnifit glass columns, yielding a volume of 7.1 mL per column. The reproducibility of the packing procedure was checked by determination of the breakthrough volume of a 1.0 M NaCl solution on each column equilibrated with 0.2 M NaCl and vice versa. The resulting breakthrough volume was 7.16 ± 0.08 mL. The porosity of the packed bed, ϵ, was assumed to be 0.4, which is near an ideal packing of spherical particles.

SMB system

The 12-column SMB was assembled by the workshop of the Kluyver Laboratory for Biotechnology, analogous to the system described by Priegnitz (1996). Streams were connected to the correct columns by four 12-port valves (Valco). An additional, 24-port valve (Valco) served as a central valve in order to establish unidirectional flow (Priegnitz, 1996). All valves were controlled by software developed in the Kluyver Laboratory for Biotechnology. Liquid was supplied to the system by two Shimadzu LC8a pumps; the extract and raffinate streams were withdrawn by two Pharmacia P-600 pumps. The actual flow rates were measured by weighing the effluent amounts that were collected during a known time interval. The concentration of salt was monitored by a Pharmacia flowthrough conductivity electrode (Pharmacia Conductivity Monitor CM-P). The dead volume of the assembled system was determined by breakthrough experiments of salt on the system without columns and was approximately 0.38 mL per column. Flow-rate ratios were corrected for the dead volume as described by Migliorini et al. (1999).

Determination of isotherm

The distribution coefficient of salt was determined from the time of the breakthrough of a stepwise change in salt concentration on individual columns, as well as on twelve columns connected in the SMB fashion. The steps in salt concentration used were 1.0 to 0.2 M as well as 0.30 to 0.22 M NaCl and vice versa. The time of breakthrough was the same as the time needed to reach half of the concentration difference.

SMB experiments

During operation of the system, the recycle stream was wasted. Before the experiment, columns were regenerated using 1.0 M NaCl and preferably reequilibrated with 0.22 M NaCl. All experiments were carried out at room temperature, without temperature control.

Numerical procedures

Breakthrough profiles were simulated using a mathematical column model programmed in Matlab. Mass transfer was included in the form of a linear driving force approximation, with an overall mass-transfer coefficient determined from relations between Stanton, Reynolds, and Schmidt dimensionless numbers (Houwing et al., 2002). The system of partial differential equations was solved by spatial discretization using the fourth-order Runge–Kutta method. The steady-state TMB profiles were computed using an equilibrium-stage model, as described in Ruthven and Ching (1989). In this model, the mass balances of all equilibrium stages were solved simultaneously using Matlab's Optimization Toolbox. The number of equilibrium stages was adjusted to match mass-transfer and dispersive effects.

Results and Discussion

Distribution coefficients

The breakthrough experiments of NaCl on a single column and 12 columns in series were fitted by a mathematical model, based on an assumption of local equilibrium. A satisfactory fit was obtained at $S = 1.09$ and $Q = 0.22$ M (cf. Figure 5). The experimental time of breakthrough at the 0.22 M to 0.30 M NaCl step was smaller than at the time of breakthrough at

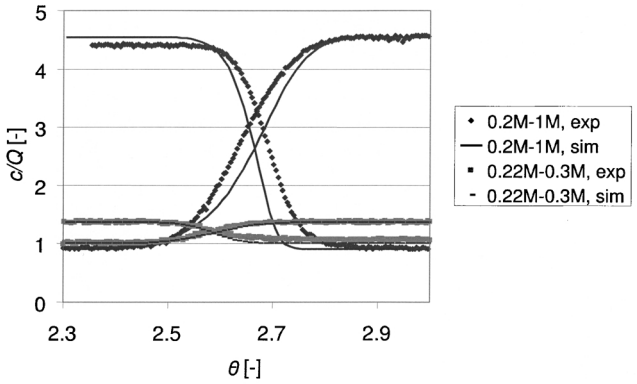

Figure 5. Experimental and simulated breakthrough of sodium chloride on 12 columns that form the laboratory-scale SMB system in series.

Predicted line: $S = 1.09$, $Q = 0.22$ M.

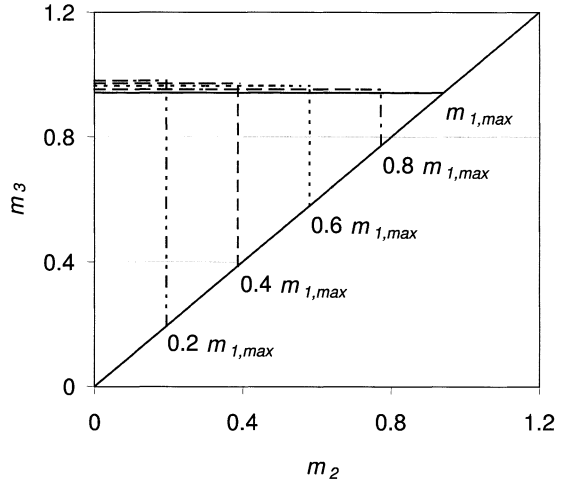

Figure 7. Influence of m_1 on the region of separation in a downward gradient.

the 0.2 M to 1.0 M NaCl step. This is in agreement with the equilibrium model, which predicts a low affinity at concentrations below Q and a higher affinity at higher concentrations (cf. Figure 2).

Operating region

Using the experimental equilibrium isotherm, an operating region has been constructed in the case of an upward and downward gradient, following the procedure outlined in the theory section (Figure 6). In the case of an upward gradient, the diffuse wave in section II sets the minimum flow-rate ratio, m_2, equal to the slope of the salt isotherm at the "slowest" desorbent concentration. The boundary on m_3 is not relevant, as the shock wave in section III always has a higher velocity than the velocity at the desorbent concentration. Hence, upward movement of this wave is already obtained at the limiting flow-rate ratio, m_2. At any point above the positive feed line, the salt wave in section III will move upward.

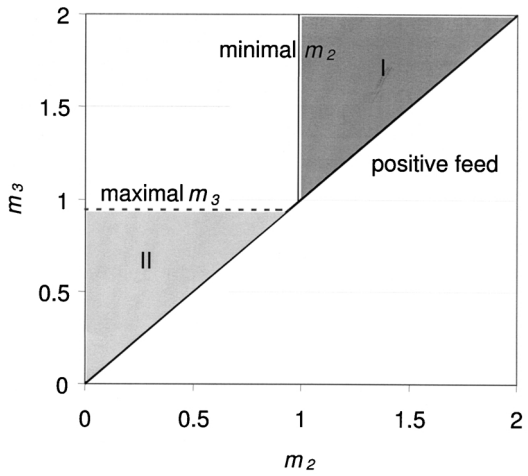

Figure 6. Operating region in an upward (I) and downward (II) gradient.

In the latter case, m_1 has been set at its maximum.

As long as m_1 is chosen well above the critical value (Table 1), its value does not influence the shape of the triangle. The concentration in section II invariably equals c_D, and the concentration in section III is determined by m_2 and the feed flow rate only. The flow rate in section IV does not influence the concentration as long as it is chosen larger than the minimal value (see Table 1). The minimal m_4 is actually smaller than the minimal m_2, because the shock wave in section IV is faster than the limiting concentration of the spreading wave in section II.

Unlike for the upward gradient, m_1 does influence the shape of the region in cases of a downward gradient, as is shown in Figure 7. Via the mass balance over the desorbent entry, Eq. 10, its value determines the concentrations in the simulated moving bed. At increasing m_1, more of the less concentrated stream is introduced, and consequently the concentrations in the SMB decrease (Figure 8). Thus, the slope and chord of the salt isotherm decrease and the region shifts to decreased m-values. Meanwhile, the maximal, m_2, is reduced at decreasing m_1. This is necessary, since the extract stream is removed per the definition, so m_2 cannot exceed m_1. This situation will frequently occur in practical situations, because eluent consumption is minimal at minimal m_1.

Obviously, m_1 has more influence on the salt concentration in bed III than it has on the concentration in bed II (Figure 8). This is expected, because the desorbent concentration is predominantly transported into sections III and IV when the gradient moves downward. At increasing m_1, more of the desorbent of lower concentration is added, so the concentration in beds III and IV decreases.

In the case of a downward gradient, the boundary on m_2 as described in Table 1 is of little importance. When m_1 is chosen at its maximum value, Eq. 10 can be used to calculate that the concentration in the top sections is close to c_D, whereas the concentration in the lower sections is close to c_F. The flow-rate ratio in section II (m_2) is then limited by the shock wave from c_F to c_D, whereas m_3 is bound by the wave velocity at c_D (Table 1). Since c_D is the lowest concentration possible, this represents the maximum velocity that can occur at this set of concentrations. The shock wave in

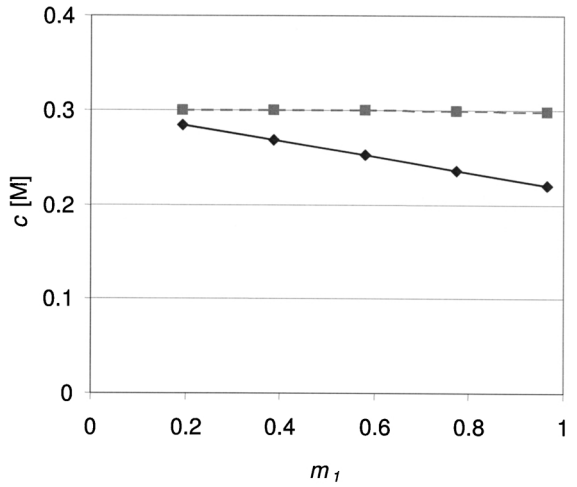

Figure 8. Influence of m_I on the salt concentrations in section I and II (■) and III and IV.

(♦) Downward gradient at $m_2 = 0.06$ and at maximal m_3, assuming TMB operation: conditions: $c_D = 0.22$ M, $c_F = 0.3$ M.

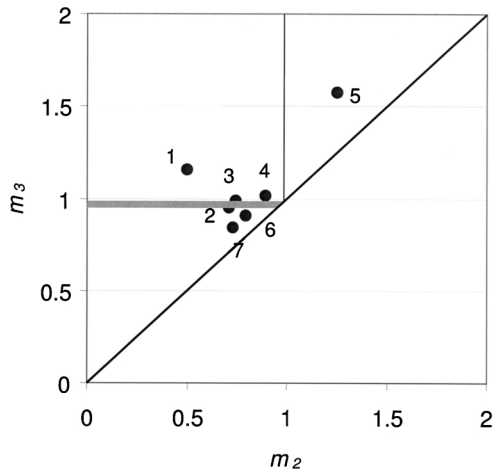

Figure 9. Position of experimental points in operating region.

Hatched boundaries indicate the range; the boundaries vary slightly per experiment due to changing m_1 and salt concentrations (see Table 2).

section II will have a lower velocity, per definition. The criterion in bed II is always met, because the necessary positive feed keeps m_2 from ever exceeding m_3. When m_1 is chosen below the maximum value, the criterion of m_2 is already met, since the bounds on m_1 and m_2 are the same.

Experimental verification

Several SMB experiments have been carried out to confirm that the correct salt profile is obtained only at flow-rate ratios inside the triangular regions. The location of the experiments inside the operating region is indicated in Figure 9, where the numbers correspond to the experiment numbers as given in Table 2. During the experiments, the concentrations in the desorbent and feed have been changed slightly, as have the values of m_1. Hence, the operating region is slightly different for each experiment. In the figure, shaded boundaries indicate the region between the maximum and minimum values during all experiments. Experiment 8 is not indicated in the figure, because fairly different salt concentrations have been used in that experiment.

The experimental conditions and observed directions of movement are shown in Table 2. Negative flow-rate ratios are a result of the dead volume in the system, which has been accounted for by using the approach of Migliorini (1999). The dead-volume effect is quite important, because the dead volume is large compared to the column volume in a laboratory-scale system. The dead-volume effect is enhanced further by the low distribution coefficient (about unity), which allows only low flow-rate ratios, especially in the case of a downward gradient.

For a prediction of direction of movement, the salt concentrations in the top and bottom sections have been calculated from the variables m, c_D, and c_F using the mass-balance equations, followed by a determination of the direction of movement using the equations shown in Table 1. In most experiments, the observed direction of movement of the salt agreed well with the predictions as is shown by the boldface type used in Table 2. In some experiments (such as experiment 1), the concentrations in the sections could not be calculated, since the experimental profile was not one of the gradient types assumed.

Table 2. Experimental Conditions and Observed Direction of Movement.

Experiment	1	2	3	4	5	6	7	8
c_D	0.22	0.22	0.22	0.22	0.3	0.22	0.22	0.27
c_F	0.3	0.3	0.3	0.3	0.22	0.31	0.31	0.15
m_1	1.12	0.95	0.93	0.98	1.56	0.95	0.88	2.11
m_2	0.50	0.71	0.75	0.89	1.25	0.80	0.73	1.12
m_3	1.15	0.95	0.98	1.01	1.57	0.91	0.84	3.07
m_4	−0.11	−0.34	−0.28	0.11	1.25	0.00	−0.05	1.09
Movement of salt in section								
I	**up**	up	**down**	**up**	**up**	up	**down**	**up**
II	**down**	**down**	**down**	**down**	**up**	**down**	**down**	**up**
III	up	**down***	up	**up**	**up**	**down***	**down**	**up**
IV	down	**down**	**down**	**down**	**up**	**down**	**down**	**up**

*No movement is predicted based on the calculated concentrations.

Note: Bold indication of the direction of movement means that the observed direction of movement agrees with the direction of movement predicted from theory.

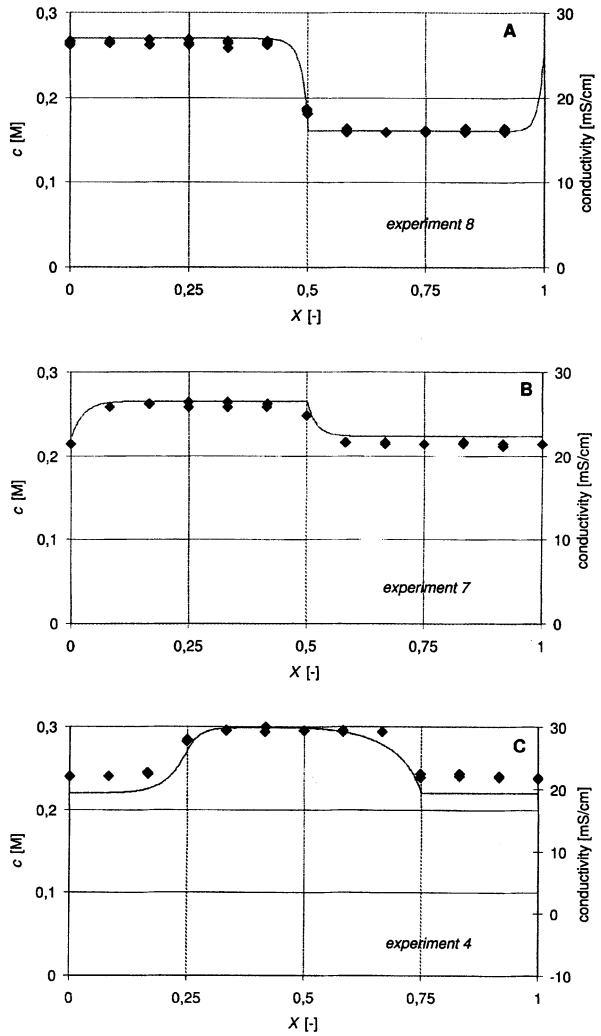

Figure 10. Simulated concentration (lines) and experimental conductivity (points) at steady state.

The experimental profiles at steady state were well predicted by an equilibrium-stage TMB model, as is shown in Figure 10, where the experimental points represent the values at the midpoint of the switch interval (cf. Ruthven and Ching, 1989). In the case of the upward gradient (experiment 8, Figure 10A), the fronts are positioned just before the outlet of the bed. This is the result of the front moving in the upward direction over the entire system; so the front "bounces" against the feed and desorbent inlet. A similar situation is seen in the case of a downward gradient (experiment 7, Figure 10B), except that the fronts are now just behind the feed and desorbent position.

Experiment 4 was positioned beside the operating region. In this experiment, both m_1 and m_3 exceeded the maximum allowed flow-rate ratio. Upward movement in section I and downward movement in section II resulted in positioning the first front between these sections. Similarly, the front between sections III and IV is a result of the upward movement in section III and downward movement in section IV (Figure 10C). The obtained gradient is neither a "top" nor a "bottom" gradient, but could be called a "center" gradient. It is of low practical value, since the high concentration of salt in the middle sections (II and III) induce a low affinity and, hence, a low throughput. Meanwhile, a high desorbent consumption is induced by the high affinity in section I.

Upward or downward gradient?

This article shows that both upward and downward gradients can be achieved. Which of the two is to be used primarily depends on the characteristics of the proteins to be separated, as will be shown in a later article. Here, we will only give some general considerations with respect to throughput and desorbent and salt consumption.

Throughput. An upward gradient is generally preferable with respect to throughput, that is, the volume of feed loaded per volume of sorbent, which is proportional to the feed flow rate $(m_3 - m_2)$. In the upward gradient, an upper limit to m_3 is absent, which enables operation at high feed flow-rate ratios (seen in Figure 6 as a long distance from the operating point to the "positive feed" line). On the contrary, the maximum m_3 is set in the downward gradient, imposed by the downward movement of salt. Hence, productivity is limited, and the use of sorbent may be considerable. It should be noted that the upward gradient SMB may have a technological limit in the (feed) flow rate, since highly asymmetrical SMBs with a low flow rate in the lower sections and an extremely high flow rate in the upper sections can hardly be operated accurately.

Desorbent and Salt Consumption. First let us focus on the absolute amount of desorbent consumed. This quantity is set by the flow-rate ratio in section I, m_{I}. In the downward gradient, m_{I} is to be smaller than the chord of the isotherm between the high concentration, c_{II}, and the low concentration, c_D (see Table 1). In the upward gradient, m_{I} is to exceed the slope of the isotherm at concentration, c_{II}, which is always larger than the chord mentioned (cf. Figure 2). Hence, the downward gradient is always operated at lower m_{I}, and, hence, the absolute consumption of desorbent is lower in the downward gradient in comparison to the upward gradient.

For a comparison of the desorbent use relative to the feed volume, we have chosen a number of gradient compositions, characterized by a fixed concentration, c_{II}, of 0.3 M NaCl, and a fixed concentration c_{III} between 0 and 0.3 M. For each of these gradients, we have computed the m-values and the required feed and desorbent concentration in both the up and downward gradients, using the mass balances and Table 1. Some additional variables are given in Table 3. The value of m_1 and m_2 have been chosen near the minimum value indicated in Table 1, thus, minimizing desorbent use and maximizing throughput. Furthermore, the salt concentration in the feed in the case of an upward gradient was chosen near the projected concentration in the top sections, which allows for a large feed flow rate and maximum throughput. To complete the analysis, the desorbent use $[= m_1/(m_3 - m_2)]$ as well as the consumption of salt $(= c_F + c_D \cdot m_1/(m_3 - m_2))$ relative to the feed volume have been calculated.

The desorbent and the salt use in an upward gradient SMB increases as difference between the bottom and top concentration increases (cf. Figure 11). This is easily explained: the larger the difference between the top and bottom concentrations, the larger the amount of feed that can be added, and

Table 3. Parameters Used in Comparison of Upward and Downward Gradient

Parameter	Value	Meaning
α_1	1.1	Ratio $m_1/m_{1,\min}$, upward gradient
α_2	1.05	Ratio $m_2/m_{2,\min}$, upward gradient
α_3	1.05	Ratio $m_{3,\max}/m_3$, downward gradient
α_4	1.05	Ratio c_{III}/c_F, upward gradient
$m_{1,\min}$	0.4	Minimal m_1, downward gradient
$m_{2,\min}$	0.1	Minimal m_2, downward gradient

the higher the throughput. Meanwhile, the desorbent flow is constant at constant c_{II}, which minimizes the ratio of desorbent to feed flow-rate ratio.

Similarly, the desorbent and salt use in the downward gradient are small for small differences in the top and bottom concentrations. Then, the salt concentration is predominantly determined by the (high) feed concentration. Hence, only a low desorbent flow rate can be applied, which favors low desorbent consumption. As the difference between the two concentrations increases, more desorbent is applied relative to the feed in order to maintain the gradient, thus increasing desorbent use.

Obviously, which of the two gradients is the most favorable with respect to desorbent or salt use strongly depends on the difference in the salt concentration between the top and bottom sections. When the difference between the two is small, the downward gradient is preferred, whereas the upward gradient is preferred when there is a large difference in salt concentration. Further optimization requires information on the proteins to be separated and is not carried out in this article.

Conclusions

Salt gradients can improve the throughput during protein separation by ion exchange in simulated moving bed. This article shows how at least four forms of the gradient can be formed. Variants include "upward" and "downward," as well as "top" and "bottom" gradients. In the less obvious downward-gradient form, the gradient forming salt moves toward the bottom of the system, due to its high affinity for the ion-exchange matrix, as well as by dead volume effects. Top gradients, with a high concentration in the top sections, are more favorable than bottom gradients with respect to throughput.

A procedure for the selection of flow rates that lead to correct positioning of both upward and downward gradients has been developed. This procedure is based on wave theory and incorporates the nonlinear Donnan isotherm of salt on an ion-exchange matrix. An operating region in the m_2-m_3 plane is identified. Correct positioning of the gradient is expected only within its boundaries. Experiments combined with mathematical modeling confirm the theoretical predictions.

Upward and downward gradients have been compared with respect to the use of desorbent and salt. When the difference in salt concentrations in the top and bottom sections is large, a downward gradient is favorable with respect to minimization of the use of desorbent and salt. When there is a small difference in gradient concentration, the upward gradient is most favorable. Further optimization requires information on the proteins to be separated.

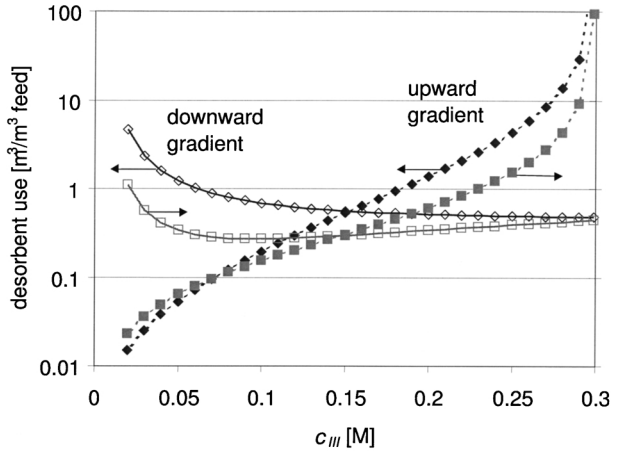

Figure 11. Desorbent use (♦) vs. salt use (■) in upward gradient (closed symbols) and downward gradient (open symbols).

In all cases, the salt concentration in the lower sections was maintained at 0.3 M. Further assumptions as shown in Table 3.

Acknowledgments

The Dutch Ministry of Economic Affairs is gratefully acknowledged for the financial support in the framework of the IOP Milieutechnologie (Preventie) program.

Notation

c = concentration in the liquid phase, kmol/m^3
F = Faraday's constant, C/mol
m = flow-rate ratio ($= \Phi_L/\Phi_S$)
q = concentration in the sorbed phase, kmol/m^3
Q = ion-exchange capacity of the resin, kmol/m^3
R = gas constant, J/mol/K
S = selectivity constant
t = time, s
T = temperature, K
v = interstitial velocity, m/s
v_s = sorbent interstitial velocity, m/s
V = volume of one column, m^3
V_d = dead volume per column, m^3
x = liquid-phase ionic fraction
X = dimensionless distance
y = sorbed-phase ionic fraction
z = ionic charge, C/mol

Greek letters

α = discrepancy parameter
β = phase ratio [$= (1-\epsilon)/\epsilon$]
ϵ = bed porosity
Φ = flow rate, m^3/s
μ = chemical potential, J
θ = dimensionless time ($t \cdot v_0/L$)
τ = switch time, s
Ψ = electrical potential, V

Super- and subscripts

0 = standard state
i = index
L = liquid
S = sorbent

Literature Cited

Ballanec, B., and G. Hotier, "From Batch to Simulated Countercurrent Chromatography," *Preparative and Production Scale Chromatography*, G. Ganetsos and P. E. Barker, eds., Dekker, New York (1993).

Helfferich, F. G., and G. Klein, *Multicomponent Chromatography: Theory of Interference*, Dekker, New York (1970).

Houwing, J., L. A. M. van der Wielen, and K. Ch. A. M. Luyben, "Development of Large Sale Purification Process for Recombinant HSA Using SMB Technology," AIChE Meeting, Los Angeles, CA (1997).

Houwing, J., H. A. H. Billiet, J. A. Wesselingh, and L. A. M. van der Wielen, "Azeotropic Phenomena During Separation of Dilute Mixtures of Proteins by Simulated Moving Bed Chromatography," *J. Chem. Technol. Biotechnol.*, **74**, 213 (1999).

Houwing, J., H. A. H. Billiet, and L. A. M. van der Wielen, "Mass Transfer Effects During Separation of Proteins in SMB by Size Exclusion," *AIChE J.*, in press (2003).

Jansen, M. L., A. J. J. Straathof, L. A. M. van der Wielen, K. Ch. A. M. Luyben, and W. J. J. van den Tweel, "A Rigorous Model for Ion Exchange Equilibria of Strong and Weak Electrolytes," *AIChE J.*, **42**, 1911 (1996).

Jensen, T. B., T. G. P. Reijns, H. A. H. Billiet, and L. A. M. van der Wielen, "Novel Simulated Moving Bed Method for Reduced Solvent Consumption," *J. Chromatog.*, **873**, 149 (2000).

Juza, M., M. Mazzotti, and M. Morbidelli, "Simulated Moving-Bed Chromatography and Its Application to Chirotechnology," *Tibtech.*, **18**, 108 (2000).

Kopaciewitz, W., M. A. Rounds, J. Fausnaugh, and F. E. Regnier, "Retention Model for High-Performance Ion-Exchange Chromatography," *J. Chromatog.*, **226**, 3 (1989).

Ma, Z., and N.-H. L. Wang, "Standing Wave Analysis of SMB Chromatography: Linear Systems," *AIChE J.*, **43**, 2488 (1997).

Mazzotti, M., G. Storti, and M. Morbidelli, "Supercritical Fluid Simulated Moving Bed Chromatography," *J. Chromatog.*, **786**, 309 (1997).

Migliorini, C., M. Mazzotti, and M. Morbidelli, "Simulated Moving Bed Units with Extra-Column Dead Volume," *AIChE J.*, **45**, 1411 (1999).

Migliorini, C., M. Wendlinger, M. Mazzotti, and M. Morbidelli, "Temperature Gradient Operation of a Simulated Moving Bed Unit," *Ind. Eng. Chem. Res.*, **40**, 2606 (2001).

Mulder, M., *Basic Principles of Membrane Technology*, Kluwer, Dordrecht, The Netherlands (1991).

Pharmacia Biotech, *Ion-Exchange Chromatography: Principles and Methods*, Västra Aros tryckeri AB9511, Sweden (1996).

Priegnitz, J. W., "Small Scale Simulated Moving Bed Separation Process," U.S. Patent No. 5,565,104 (1996).

Rhee, H.-K., R. Aris, and N. R. Amundson, "Multicomponent Adsorption in Continuous Countercurrent Exchangers," *Philos. Trans. Roy. Soc. London, Ser. A*, **269**, 187 (1971).

Ruthven, D. M., and C. B. Ching, "Countercurrent and Simulated Countercurrent Adsorption Separation Processes," *Chem. Eng. Sci.*, **44**, 1011 (1989).

Storti, G., M. Masi, S. Carrà, and M. Morbidelli, "Optimal Design of Multicomponent Countercurrent Adsorption Separation Processes Involving Nonlinear Equilibria," *Chem. Eng. Sci.*, **44**, 1329 (1989).

Storti, G., M. Mazzotti, M. Morbidelli, and S. Carrà, "Robust Design of Binary Countercurrent Adsorption Separation Processes," *AIChE J.*, **39**, 471 (1993).

Van Walsem, H. J., and M. C. Thompson, "Simulated Moving Bed in the Production of Lysine," *J. Biotechnol.*, **59**, 127 (1997).

Manuscript received Apr. 2, 2001, and revision received Aug. 27, 2002.